

OPTIMIZATION OF CHESSBOARD SCANNING STRATEGY USING GENETIC ALGORITHM IN MULTI-LASER ADDITIVE MANUFACTURING PROCESS

Ehsan Malekipour¹, Homero Valladares², Yung Shin²

¹Department of Mechanical Engineering, University of Michigan, Ann Arbor, MI 48109, USA

²School of Mechanical Engineering, Purdue University West Lafayette, IN 47907, USA

Hazim El-Mounayri³

³Purdue School of Engineering and Technology
Indianapolis, IN 46202, USA

ABSTRACT

Residual stress and manufacturing time are two serious challenges that hinder the widespread industry adoption and implementation of the powder-bed fusion (PBF) process. Commercial Multi-Laser PBF (ML-PBF) systems have been developed by several vendors in recent years, which dramatically increase the production rate by employing more heat sources (up to 4 laser beams). Although numerous research works conducted toward mitigation of the effects of residual stress on printed parts in the Single Laser PBF (SL-PBF) process, no research work on this topic has been reported for the ML-PBF process to date.

One of the most efficient real-time approaches to mitigate the influence of residual stress and as such the process lead time effectively is to improve the scanning strategy. This approach can be also implemented effectively in the ML-PBF process. In this work, we extend the previously developed GAMP (Genetic Algorithm Maximum Path) strategy for optimizing the scanning path in ML-PBF. The E-GAMP (the Extended GAMP) strategy manipulates the printing topology of the islands and generates more thermally efficient scanning patterns for the chessboard scanning strategy in ML-PBF. This strategy extends the single thermal heat source to multiple ones (2 as well as 3 lasers). To validate the effectiveness of the proposed strategy, we simulate the thermal distribution throughout a simple rectangular layer by ABAQUS for both the traditional successive scanning strategy and the E-GAMP strategy. The results demonstrate that the E-GAMP strategy considerably decreases the manufacturing time while it reduces the maximum temperature gradient, or in other words, generates a more uniform temperature distribution throughout the exposure layer.

Keywords: Multi-laser Powder-bed fusion process; metal additive manufacturing; scanning strategy optimization; chessboard scanning strategy; genetic algorithm; temperature distribution

1. INTRODUCTION

1.1 Background

Traditionally, one obstacle for more widespread usage of metal additive manufacturing (MAM) was the considerably longer production time compared to traditional manufacturing

processes. More recently, multi-laser / multi scanner systems have offered an attractive solution to overcoming the productivity challenge. This new process can offer production rates multiple of those achieved on single-laser systems, print different sections (such as support structure vs the main part) with different ultimate layer thickness due to access different laser powers, and enable future multi-material printing. At the end of 2013, SLM Solutions presented SLM 500HL which is equipped with a multi-laser / multi-scanner system with up to 4 lasers and 4 scanners. Using 4 lasers reduced the printing time of each layer by 75% (see Figure 1) [1].

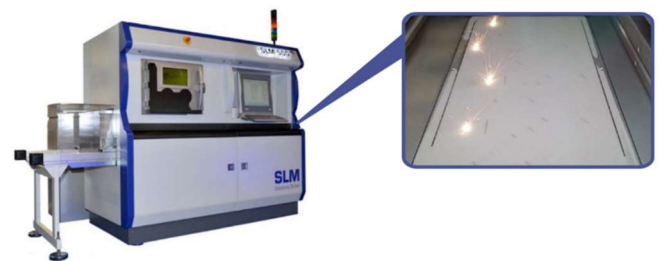


FIGURE 1: SLM 500 HL WITH UP TO 4 LASER / 4 SCANNER PRODUCTION CAPABILITY

Masoomi et al. [2] in 2017, conducted a simulation to study the effects of using multiple lasers on the sintered part integrity compared with using a single heat source. To fulfill such objective, they studied the spatiotemporal temperature fields/gradients throughout 16 static points in two consecutive layers and different scanning strategies in the SL- and ML- PBF processes. The radar charts in Figure 2 visualize the uniformity in temperature gradients along with each layer in 16 different points. Different scanning strategies use either one laser (S1-S2, S5-S6, and S9) or four lasers and the strategies print either the entire zone as a single entity (S1 and S5), four islands (S2-S7, S9-S11), or four adjacent stripes with a different combination of track directions (x- or y- direction) (see Figure 3). The authors demonstrated that the employment of chessboard scanning strategy with multiple lasers reduce the average magnitude of peak temperature gradients experienced, and thus the general level of residual stress expected, along with a layer. However, they reported that such strategies can result in non-uniform,

¹ Corresponding author: emalekip@umich.edu

anisotropic residual stress distributions in printed parts, which ultimately affecting its mechanical properties. In this work, the simulation was limited to only 4 adjacent islands.

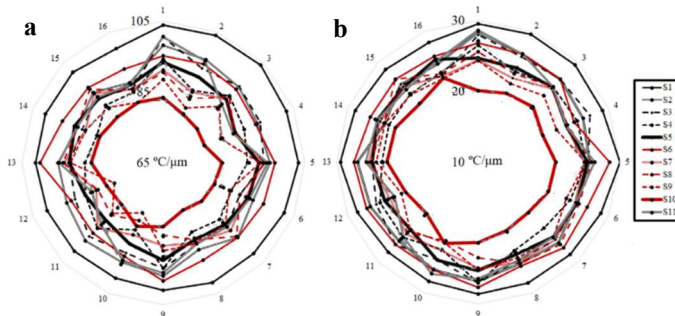


FIGURE 2: RADAR CHART SHOWING THE MAXIMUM TEMPERATURE GRADIENTS MEASURED AT POINTS P1-P16 SCANS BY THE SCAN STRATEGIES S1-S11 FOR A. THE FIRST LAYER AND B. THE SECOND LAYER [2]

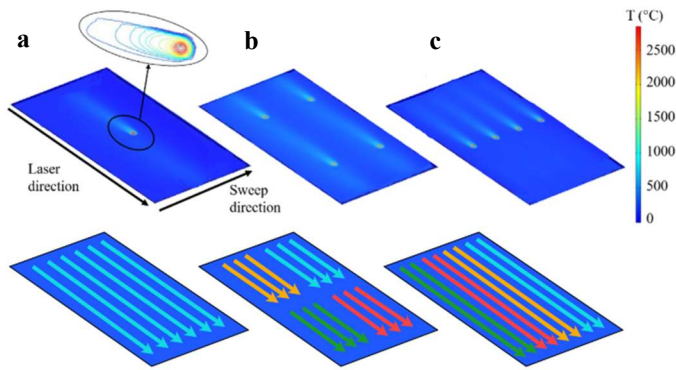


FIGURE 3: SCAN STRATEGIES AND THE SIMULATED TEMPERATURE FIELDS IN SL- AND ML- PBF PROCESSES FOR A. A SINGLE LAYER; B. FOUR ISLANDS; AND C. FOR STRIPS [2]

Despite the great capabilities and potential of this process, the development or optimization of different scanning strategies for mitigation of the potential thermal abnormalities has not been attempted. Also, the study of thermal interaction between different printed sections of an exposure layer is lacking. In this work, we apply the Genetic Algorithm (GA) for optimization of the chessboard scanning strategy for multi-laser MAM. This was achieved by modifying and expanding a previously developed scanning strategy, GAMP (Genetic Algorithm Maximum Path) [3]. The extended strategy called the E-GAMP strategy can also be applied to ML-PBF.

1.2 Problem description

The literature introduces different methods to mitigate the effects of residual stress on the part printed by the PBF process. These methods include preheating of powder-bed, rescanning the printed layer, manufacturing of support structure, post-processing heat treatment, and manipulation of the scanning strategy. However, preheating and rescanning strategies decrease

energy efficiency and increase manufacturing time and total manufacturing cost [4, 5]. The manufacturing of support structures significantly depends upon the designer's experience and increases the manufacturing time as well as the material usage [6]. Heat treatment can reduce the residual stress up to 70% as reported by Shiomi et al. [7], however, it is incapable to reverse the effects of residual stresses on distortions, delamination, and stress-related cracking that occur during the manufacturing process [5]. One of the most attractive real-time methodologies to mitigate the influence of the residual stress effectively is scanning strategy improvement. Scanning strategy refers to the manipulation of laser specifications, scanning pattern, and the topology of scanning zones such as modification of the printing order of the islands in the chessboard scanning strategy [5, 8, 9]. The objective for manipulation of the scanning strategy is to generate relatively more uniform temperature distribution, in other words, lower generated temperature gradient, compared with the traditional strategies throughout the printed part [8]. The thermal gradient between different printed zones throughout a layer or between different printed layers (in additive orientation) causes thermal stress and as a result, different thermal abnormalities such as cracks, distortion, warpage, etc. [10, 11] (see Figure 4). In this work, I introduce a new scanning strategy for manipulation of the scanning topology of the islands in the chessboard scanning strategy in the ML-PBF process.



FIGURE 4: DISTORTION DUE TO NON-UNIFORM TEMPERATURE DISTRIBUTION [12]

2. METHODOLOGY

In this work, we extend the previously developed strategy for the case of one laser [3] to one that considers 2 and 3 lasers. The objective is to introduce a scanning strategy that generates a more uniform temperature distribution compared to the traditional strategies. Two main constraints are considered for the development of the strategy. First, the generation of the maximum path by developing the GAMP strategy for each printed sub-layer [3] and second, the minimum allowable distance between the multiple heat sources to avoid Heat Affected Zones (HAZ) while printing different sub-layers.

2.1 Satisfying the first constraint

To maximize the scanning path in each exposure sub-layer, the path that connects the centers of the islands is maximized using GA. This method maximizes the cooling time for the islands, reduces the chance of heat accumulation zones

throughout a layer, and produces relatively more uniform temperature distribution. A rectangular exposure layer is printed by one, two, and three lasers. The lasers print the entire layer, two sub-layers, and three sub-layers, respectively (see Figure 5). The resulted temperature distribution is simulated using ABAQUS and compared with the traditional successive scanning strategy [5].



FIGURE 5: SPLITTING A LAYER TO TWO AND THREE SUB-LAYERS FOR PRINTING BY THE ML-PBF PROCESS

2.2 Satisfying the second constraint

Price et al [13] showed that a heat source can affect a maximum of 8 mm thermally on adjacent areas (when we are printing an overhang zone) in PBF (see Figure 6). This constraint will be applied as the second constraint to optimize the scanning strategy while we use more than one heat source simultaneously for printing different sub-layers.

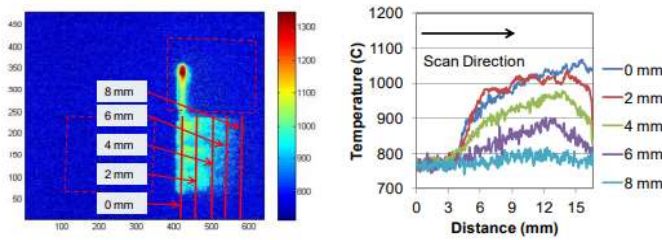
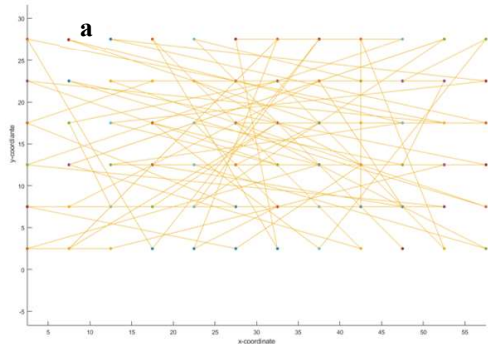


FIGURE 6: A. HEAT AFFECTED ZONES; B. AVERAGE TEMPERATURE PROFILE FOR AN OVERHANG LAYER [13]

2.3 E-GAMP strategy

The following flowchart shows the main steps in the E-GAMP strategy. This strategy firstly splits the entire layer to different sub-layers according to the number of lasers in the system and the geometry of the layer. Then, the algorithm reads the centers of the islands in each sub-layer in order to calculate the distance between separate pairs of islands. In the next step, different paths are generated randomly and used as the initial



population for the GA algorithm. Each path contains the centers of all the islands that are connected with no repetitive root between any pair of islands. The code generates the maximum total path that connects all the islands in each separate sub-layer. The total path is the sum of the separate paths in different sub-layers. Finally, the algorithm provides us with the sequence of the islands for each sub-layer, namely, the printing order of the islands to be sent to the controller (the ASCII file).

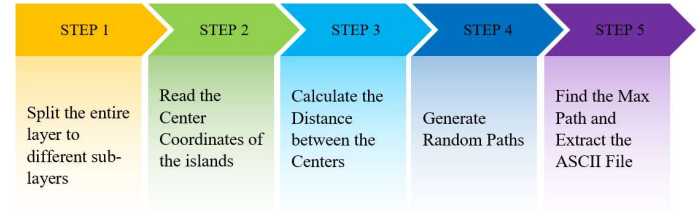


FIGURE 7: DIFFERENT STEPS OF THE E-GAMP STRATEGY

3. RESULTS AND DISCUSSION

3.1 Implementation of the E-GAMP strategy

In this section, we apply the E-GAMP strategy to a layer with dimensions 40 mm \times 70 mm. The layer, which includes 6 islands along the width and 12 islands along the length, is printed by one, two, and three lasers for the entire layer, two sub-layers, and three sub-layers, respectively. The strategy provides the optimized scanning path (or the optimized printing order of the islands) for the entire layer, two, and three sub-layers in Figures 8, 9, and 10, respectively. The simulation of temperature distribution generated by each path is presented in sub-section 3.2 and the results are compared with the temperature distribution of traditional successive scanning strategy for SL-PBF. Figure 8 shows the generation of the maximum path by the implementation of the developed E-GAMP strategy for the entire layer. Figure 9 shows the generation of the maximum path by the implementation of the developed E-GAMP strategy for two sub-layers. As depicted, the neighbor islands in the separated sub-layers (the islands adjacent to the dashed red line), are printed in different time steps to satisfy the second constraint. This means that two adjacent islands in two different sub-layers are never printed simultaneously to keep the minimum allowable distance between the lasers and avoid HAZ during the printing process.

FIGURE 8: A. THE GENERATED PATH BY THE E-GAMP STRATEGY FOR THE ENTIRE LAYER; B. THE PRINTING ORDER OF THE ISLANDS

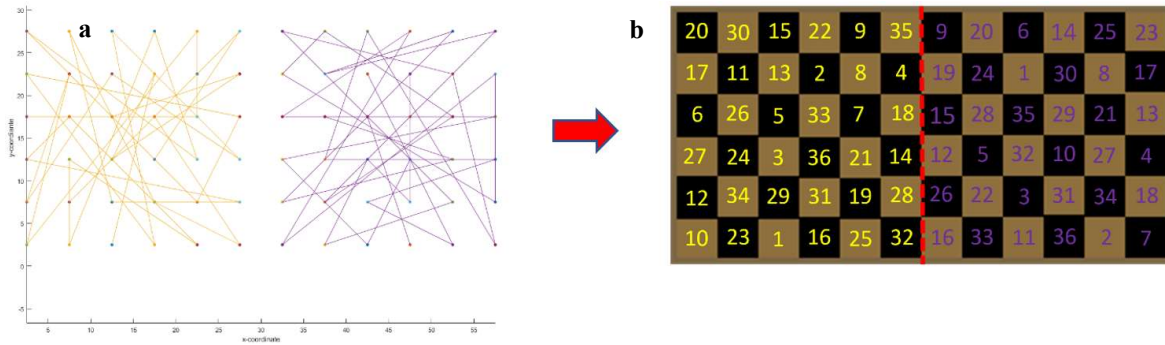


FIGURE 9: A. THE GENERATED PATH BY THE E-GAMP STRATEGY FOR TWO SUB-LAYERS; B. THE PRINTING ORDER OF THE ISLANDS

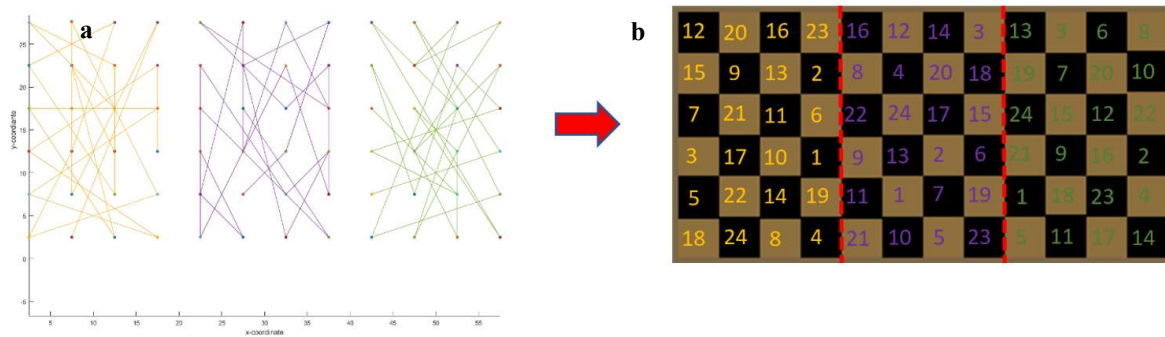


FIGURE 10: A. THE GENERATED PATH BY THE E-GAMP STRATEGY FOR THREE SUB-LAYERS; B. THE PRINTING ORDER OF THE ISLANDS

Figure 10 shows the generation of the maximum path when the E-GAMP strategy is implemented for three sub-layers. Figure 10.a illustrates how the algorithm resulted in paths connecting the islands with longer distances in between to produce the maximum path in each sub-layer. Figure 10.b also shows the neighbor islands in the separated sub-layers (the islands adjacent to the dashed red lines), are printed in different time steps to satisfy the second constraint and avoid HAZ in the ML-PBF process.

3.2 Validation with simulation

3.2.1 Temperature distribution analysis

In this section, we employ FALS TECHS, our simulation technique developed in ABAQUS for simulation of temperature distribution throughout the layers printed in the chessboard scanning strategy [14] to validate the effectiveness of the E-GAMP scanning strategy and compare its prediction of the temperature distribution with its counterpart from traditional successive scanning strategy. We model a simple rectangular cube to investigate the effects of different strategies. This cube transfers heat with convection through the top surface and all the other faces are assigned a constant temperature of 296.15 K to

simulate the conduction heat transmission between the cube faces and the testbed compartment. The initial temperature of 603.15 K is considered for the previously printed layers with a height of 2.95 mm, and the top layer is SS 316L material powder with a thickness of 20 μm . Figure 11 shows the model specifications.

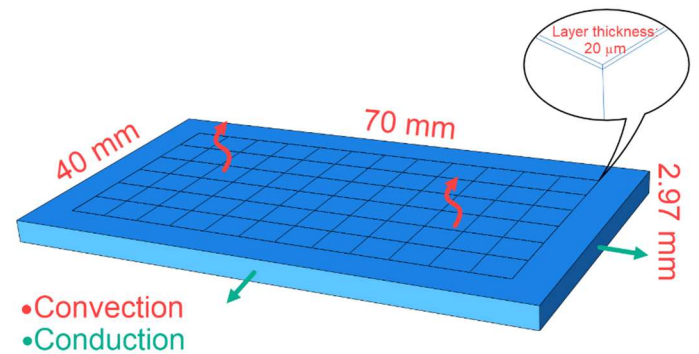


FIGURE 11: THE MODEL SPECIFICATIONS AND THERMAL TRANSMISSION WITH THE SURROUNDING ENVIRONMENT

As Figure 12 demonstrates, the E-GAMP strategy (Figures 12.b, 12.c, and 12.d) scans the islands throughout different zones of the entire layer, instead of printing all the islands successively (Figure 12.a). As Figure 13 demonstrates, the scattering of the printed islands leads to a lower temperature gradient throughout the layer. In this figure, the first and second diagrams of each row show the temperature variations along the reference path (marked in Figure 12.a), in half as well as the final scanning time of the layer. Furthermore, the third diagram of each row shows the temperature variation of the reference point (marked in Figure 12.a) versus the entire scanning time. Comparing the temperature variation along the reference path in the successive and single laser E-GAMP scanning strategy (Figures 13.a vs. Figure 13.d for half scanning time and Figure 13.b vs. Figure 13.e for the total scanning time) shows that the maximum temperature gradient decreased to 4.28 K and 4.56 K, respectively. Also, the diagrams are converging to plateau. Furthermore, the reference point, allocated on one side of the printing layer, shows a lower temperature gradient during the printing process (Figure 13.c vs. Figure 13.f). The lower temperature gradient in the E-GAMP strategy means a relatively more uniform temperature distribution compared with the successive scanning strategy.

As Figure 12.c and 12.d shows, in general, increasing the number of heat sources also helps in the scattering of temperature

more uniformly throughout the layer. For instance, the trend in Figures 13.c, 13.f, 13.i, and 13.l also corroborates that increasing the number of heat sources helps decrease the maximum temperature gradient in the reference point from 92.58 K to 47.88 K. However, Figure 14 shows that increasing the number of heat sources increases the total temperature value throughout the exposure layer. This phenomenon indicates the higher chance of generation of heat accumulation zones during the ML-PBF process. In the FALS TECHS simulation [14], the temperature values in the legends (Figure 14) represent the average temperature of the islands and not the melt pool. The temperature variation along the reference path resulting from two and three lasers E-GAMP strategies (Figures 13.g, 13.h, 13.j, and 13.k) also shows the convergence of the temperature variations toward a plateau; however, due to the presence of printed islands adjacent to the selected path, the temperature gradient shows a higher temperature gradient at the selected moments.

Compared to the random chessboard scanning strategy [5], the E-GAMP scanning strategy increases the time elapses between the scanning of the islands as well as decreases the chance of scanning two adjacent islands successively. These factors decrease the possibility of heat accumulation in different exposure zones during the printing process. Furthermore, as Figure 12 shows, the ML-PBF process considerably decreases the printing time (in this case, from 5.8 sec to 1.9 sec).

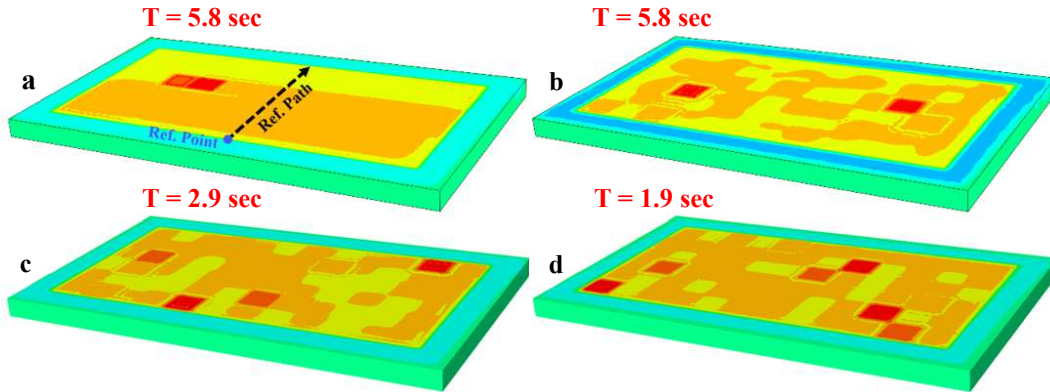
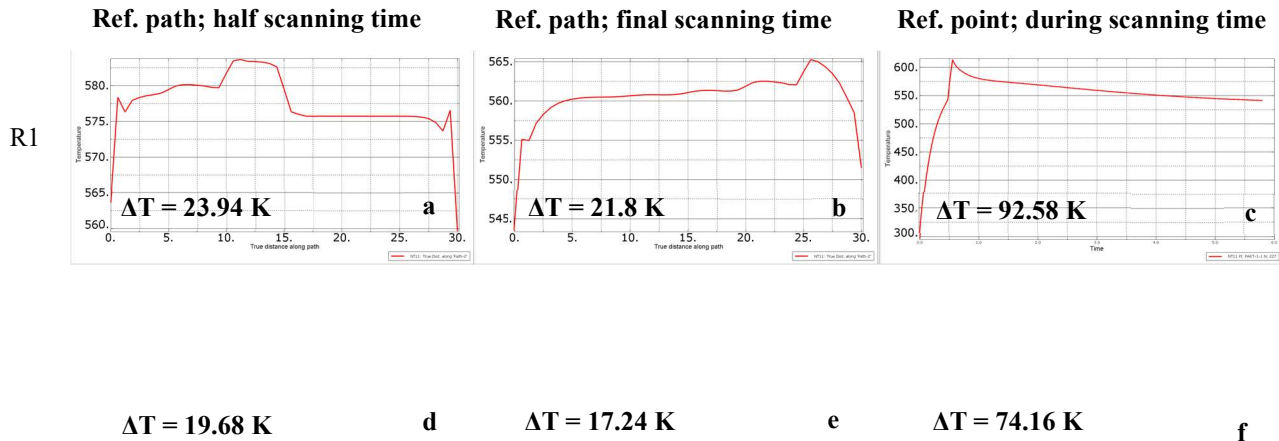


FIGURE 12: TOTAL SCANNING TIME AND TEMPERATURE FIELD GENERATED IN A RANDOM TIME FRAME BY DIFFERENT STRATEGIES: A. SUCCESSIVE; B. E-GAMP WITH ONE LASER FOR THE ENTIRE LAYER; C. E-GAMP WITH TWO LASERS FOR TWO SUB-LAYERS; D. E-GAMP WITH THREE LASERS FOR THREE SUB-LAYERS



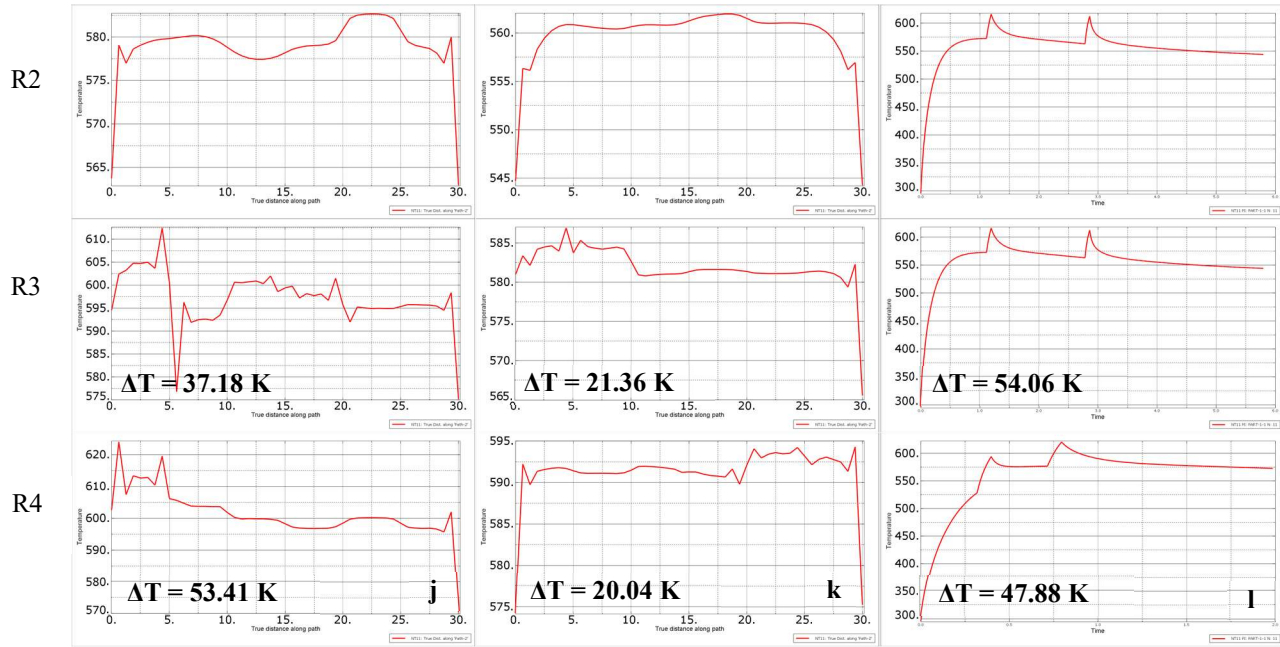


FIGURE 13: TEMPERATURE VARIATION FOR R1. SUCCESSIVE SCANNING STRATEGY, R2. SINGLE-LASER, R3. TWO-LASERS, AND R4. THREE LASERS SCANNING STRATEGIES

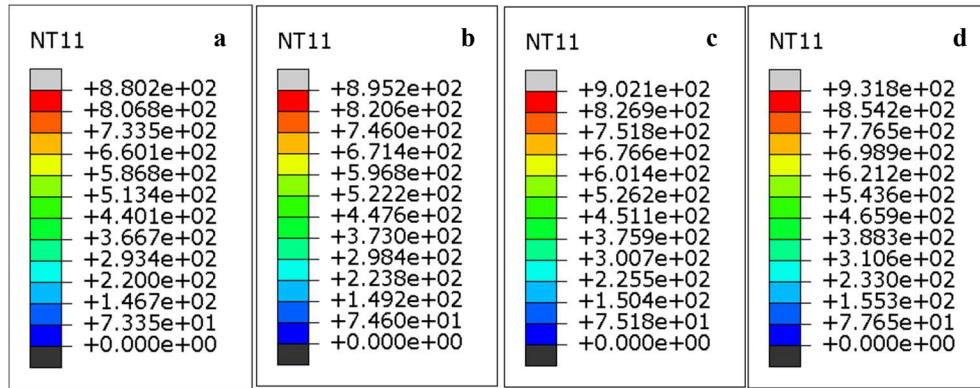


FIGURE 14: TEMPERATURE LEGEND FOR DIFFERENT SCANNING STRATEGIES: A. SUCCESSIVE; B. E-GAMP WITH ONE LASER; C. EGAMP WITH TWO LASERS; D. E-GAMP WITH THREE LASERS

4. Conclusion and future work

ML-PBF process can considerably increase the production rate. The results show that this process decreases the printing time 67% compared to SL-PBF; nonetheless, there is no research on modifying the scanning strategy for this process. In this paper, we developed and evaluated a new scanning strategy, namely E-GAMP strategy, for modifying the printing order of islands in ML-PBF. The E-GAMP strategy produces temperature distribution that is relatively more uniform, increases the cooling time, and reduces the chance of developing heat accumulation zones compared to the traditional chessboard scanning strategies. The simulation results demonstrated a decrease in the maximum temperature gradient for a reference point from 92.58 K using traditional successive scanning strategies to 47.88 K

using the new strategy. The effectiveness of this strategy on making the temperature distribution uniform is also corroborated by the general trend of the temperature profiles which converge to a plateau throughout the printed layer when using the E-GAMP strategy. In addition, the results showed that using multiple heat sources in ML-PBF increases the ultimate temperature value, which increases the chance of heat accumulation compared to the SL-PBF. This issue was addressed and handled successfully by imposing a minimum allowable distance constraint between different heat sources during the printing strategy.

Finally, it should be noted that some of the steps in the E-GAMP algorithm, including splitting a layer to different sub-layers, reading the coordinates, and extracting the ASCII file for

sending to the controller, are operated manually. Further work is needed to achieve a fully automatic approach.

REFERENCES

- [1] Wiesner, A. and D. Schwarze. *Multi-laser selective laser melting*. in *8th International Conference on Photonic Technologies LANE*. 2014.
- [2] Masoomi, M., S.M. Thompson, and N. Shamsaei. *Quality part production via multi-laser additive manufacturing*. *Manufacturing Letters*, 2017. **13**: p. 15-20.
- [3] Malekipour, E., Y.C. Shin, and H. El-Mounayri. *Optimization of Chessboard Scanning Strategy by Using Genetic Algorithm in Powder-bed Fusion Process*. 2020.
- [4] Papadakis, L., D. Chantzis, and K. Salonitis, *On the energy efficiency of pre-heating methods in SLM/SLS processes*. *The International Journal of Advanced Manufacturing Technology*, 2018. **95**(1-4): p. 1325-1338.
- [5] Mugwagwa, L., et al., *Evaluation of the impact of scanning strategies on residual stresses in selective laser melting*. *The International Journal of Advanced Manufacturing Technology*, 2019. **102**(5-8): p. 2441-2450.
- [6] Malekipour, E., A. Tovar, and H. El-Mounayri, *Heat Conduction and Geometry Topology Optimization of Support Structure in Laser-Based Additive Manufacturing*, in *Mechanics of Additive and Advanced Manufacturing, Volume 9*. 2018, Springer. p. 17-27.
- [7] Shiomi, M., et al., *Residual stress within metallic model made by selective laser melting process*. *CIRP Annals*, 2004. **53**(1): p. 195-198.
- [8] Malekipour, E. and H. el-Mounayri, *Scanning Strategies in the PBF Process – A Critical Review*. 2020.
- [9] Marrey, M., et al., *A framework for optimizing process Parameters in powder bed fusion (PBF) process using artificial neural network (ANN)*. *Procedia Manufacturing*, 2019. **34**: p. 505-515.
- [10] Malekipour, E. and H. El-Mounayri, *Common defects and contributing parameters in powder bed fusion AM process and their classification for online monitoring and control: a review*. *The International Journal of Advanced Manufacturing Technology*, 2018. **95**(1-4): p. 527-550.
- [11] Malekipour, E. and H. El-Mounayri, *Defects, process parameters and signatures for online monitoring and control in powder-based additive manufacturing*, in *Mechanics of Additive and Advanced Manufacturing, Volume 9*. 2018, Springer. p. 83-90.
- [12] *3D Printing Opens Up New Dimensions*. 2019; Available from: www.spotlightmetal.com.
- [13] Price, S., et al. *Experimental temperature analysis of powder-based electron beam additive manufacturing*. in *24th Annual International Solid Freeform Fabrication Symposium, Austin, TX*. 2013.
- [14] Malekipour, E., et al., *An Innovative Fast Layer-wise Simulation of Temperature distribution using a Chessboard Strategy (FALS TECHS) in the Powder-bed Fusion Process*. *Additive Manufacturing*, 2020.

1. Finalizing the template
2. Subnut to NAMRC 49